Catalysis
Science & Technology

Cite this: *Catal. Sci. Technol.*, 2011, **1**, 601–608

www.rsc.org/catalysis

PAPER

Low temperature CO oxidation on Cu–Cu_2O/TiO_2 catalyst prepared by photodeposition

Guangjun Wu, Naijia Guan and Landong Li*

Received 28th January 2011, Accepted 31st March 2011
DOI: 10.1039/c1cy00036e

A series of Me/TiO_2 samples (Me = V, Cr, Mn, Fe, Co, Ni, Cu and Zn) with designed $Me:TiO_2$ ratio of 1 : 10 were prepared by a photodeposition method and studied for the oxidation of CO. The Cu/TiO_2 catalyst exhibited remarkably high activity and an overall CO oxidation could be achieved at <100 °C. The effects of activation temperatures, GHSV and initial CO concentration on CO oxidation over Cu/TiO_2 were further investigated. XRD, TEM, XPS-AES, H_2-TPR and FTIR of CO adsorption were employed to characterize Cu/TiO_2 samples and the exact composition of Cu/TiO_2 prepared by photo-deposition was determined to be Cu–Cu_2O/TiO_2. Based on the catalytic and characterization results, the possible mechanism for CO oxidation over Cu–Cu_2O/TiO_2 was discussed. Finally, the durability and deactivation of Cu–Cu_2O/TiO_2 during CO oxidation was investigated in time-on-stream reaction.

Introduction

The catalytic oxidation of carbon monoxide to carbon dioxide is one of the most studied reactions in environmental catalysis due to its great significance not only in fundamental heterogeneous catalysis but also in industrial application. In the research of catalysts for CO oxidation, precious metals, *e.g.* Au[1–3] and Pd,[4,5] have been found to be highly active even at very low temperatures and thus receive much attention. The catalyst preparation, catalytic studies and mechanism aspects of CO oxidation on precious metals have been investigated in details. Although precious metal catalysts show remarkable activity for CO oxidation, the high cost of precious metal materials restricts the application of these catalysts to a great extent. To address this concern, transition metal catalysts are being investigated as less expensive candidates for CO oxidation. Cobalt catalysts have been found to be highly active for CO oxidation and their activities are almost comparable with precious metal catalysts.[6–10] However, cobalt catalysts are easily deactivated during the reaction, probably originated from the surface reconstruction process.[6,7] Especially, cobalt catalysts are extremely sensitive to the presence of water, which leads to serious deactivation by blocking the reactive sites.[10]

During past decades, copper catalysts (Cu–Cu_2O–CuO system) have been extensively studied as eligible catalysts for a number of heterogeneous reactions, *e.g.* water–gas shift reaction and NO_x elimination. Researches on CO oxidation over copper catalysts have also been carried out in the early studies where the kinetics and mechanism aspects are focused.[11–13] Recently, the oxidation of CO over copper catalysts is re-visited due to the persistent interest in this reaction and more important, the outstanding CO oxidation activity of copper catalysts just revealed.[14–19] White *et al.* developed a catalyst system comprised of Cu_2O nanoparticles supported on silica gel that exhibited exceptional activity toward CO oxidation.[14] Theoretical calculations suggested that lattice oxygen play a critical role in the CO oxidation process, verifying the Langmuir–Hinshelwood mechanism. Chen *et al.* demonstrated that Cu/TiO_2 prepared by wet impregnation was highly active for CO oxidation and they proposed that isolated Cu^{2+} was the main factor determining the activity.[15] Wan *et al.* found CO pretreatment to be a feasible means to promote the activity of Cu/Al_2O_3 for CO oxidation and an overall CO oxidation could be obtained at *ca.* 200 °C on the best catalyst.[16] They further proposed that the dispersed Cu^+ originated from the reduction of dispersed Cu^{2+} played a significant role in low temperature CO oxidation. In the work of Cao *et al.*, mesoporous copper catalysts, CuO–Fe_2O_3[17] and CuO–$Ce_{0.8}Zr_{0.2}O_2$,[18] were prepared by surfactant-assisted nanoparticles assembly. The mesoporous copper catalysts exhibited extremely high activity and total oxidation of CO could be achieved at *ca.* 100 °C.

Even though copper catalysts have been recognized as promising candidates for low temperature CO oxidation, the catalytic activities reported on copper catalysts are somewhat contradictory. Many aspects on the complex Cu–Cu_2O–CuO system are to be studied and first of all, it is quite desired to analysis the key factor controlling the activity of copper catalysts. In this work, we will present a comprehensive study

Key Laboratory of Advanced Energy Materials Chemistry (Ministry of Education), College of Chemistry, Nankai University, Tianjin 300071, P. R. China. E-mail: lild@nankai.edu.cn; Fax: +86-22-23500341; Tel: +86-22-23500341

on CO oxidation over Cu/TiO_2 prepared by photodeposition and wet impregnation. The as-prepared Cu/TiO_2 samples are characterized by a series of techniques and the composition and oxidation states of copper are well defined. Based on the characterization and catalytic results, the CO oxidation mechanism over Cu/TiO_2 prepared by photodeposition is carefully discussed.

Experimental

Preparation of Me/TiO_2 catalyst

Commercial TiO_2 (Degussa P25, 70% anatase, 30% rutile) was used as support and Me/TiO_2 (Me = V, Cr, Mn, Fe, Co, Ni, Cu and Zn) catalysts with $Me:TiO_2$ ratio of 1 : 10 were prepared by so-called photodeposition method.[20,21] In a typical synthesis of Cu/TiO_2, 100 mL 2 mM $Cu(NO_3)_2$ solution, 160 mg of TiO_2 and 10 mL of ethanol were added into a round-bottom quartz flask under vigorous stirring to form slurry. The slurry was adjusted to pH = 9.5 ± 0.5 using either 1 M HCl or 1 M NaOH aqueous solution and irradiated by a high-pressure mercury light with the main wavelength of 365 nm for 6 h under the protection of pure nitrogen. Finally, the particles were filtered, dried at ambient conditions and denoted as Cu/TiO_2-ph. The exact Cu loading in Cu/TiO_2-ph is 7.05%, as determined by ICP analysis.

For reference, Cu/TiO_2 with $Cu:TiO_2$ ratio of 1 : 10 was also prepared by wet impregnation and the obtained sample was denoted as Cu/TiO_2-im (Cu loading: 7.21%).

Catalyst characterization

The X-ray diffraction patterns of samples were recorded on a Rigaku powder diffractometer (D/MAX-RB) using Cu-Kα radiation (λ = 0.15418 nm) at a scanning rate of 4° min^{-1} in 2θ = 10–80°.

X-Ray photoelectron and Auger electronic spectra were recorded on a Quantum-ESCA spectrometer with a pass energy of 20 eV and monochromated Mg-Kα X-ray source. Accurate binding energies (±0.1 eV) were determined with respect to the position of the adventitious C 1s peak at 284.6 eV.

Transmission electron microscopy (TEM) images of samples were acquired on a Tecnai G^2 2010 S-TWIN transmission electron microscope at an accelerate voltage of 200 kV.

The temperature-programmed reduction experiments of samples were carried out on a chemisorption analyzer (Chemisorb 2720, Micromeritics) with 5 vol% H_2/Ar at a heating rate of 10 °C min^{-1} from room temperature to 500 °C. Prior to reduction, the sample (100 mg) was pretreated in He at 400 °C for 1 h.

FTIR spectra of CO adsorption on Cu/TiO_2 catalysts were collected on the spectrometer (Bruker Tensor 27) with 128 scans at a resolution of 4 cm^{-1}. A self-supporting pellet (*ca.* 0.05 g) made of sample was placed in the IR flow cell and the reference spectrum (*i.e.* background spectrum) was taken at room temperature. After the He stream was switched to a gas mixture containing 1% CO in He at a total flow rate of 30 mL min^{-1}, a series of time-dependent FTIR spectra of CO adsorption on the samples were sequentially recorded.

Catalytic oxidation of carbon monoxide

The catalytic oxidation of CO was performed in a fixed-bed flow microreactor at atmospheric pressure. Typically, 0.2 g sample (sieve fraction of 0.16–0.25 mm) was placed in a quartz reactor (4 mm i.d.) and activated in reactant gas mixture (5000 ppm CO in air) at desired temperature for 1 h. After cooling to room temperature in air, the reactant gas mixture (5000 ppm CO in air) was fed to the reactor. The total flow rate of the gas mixture was kept at 80 mL min^{-1}, corresponding to a GHSV of 24 000 h^{-1}. The inlet and outlet gases were monitored on-line using a gas chromatograph (HP 6820 series) equipped with molecular sieve 5A and Porapak Q columns. The CO conversion was calculated both from the consumption of CO and the production of CO_2 in the outlet.

For kinetics study, 0.05–0.15 g sample (sieve fraction of 0.16–0.25 mm, small enough to exclude mass transfer limitations) was employed and the total flow rate of the gas mixture (5000 ppm CO, air balance) was fixed at 80 mL min^{-1}. The reactor was well approximated as an isothermal plug-flow reactor and the CO conversion was restricted to below 15% to ensure that the data obtained were differentiated. The kinetic data were acquired after 60 min of steady-state reaction and the first data point was well duplicated after each kinetic run.

In situ FTIR study on CO oxidation

In situ FTIR studies were performed using a Bruker Tensor 27spectrometer with 256 scans at a resolution of 4 cm^{-1}. All samples were used as self-supporting wafers (*ca.* 0.05 g) and pretreated in He at 400 °C for 1h prior to experiments. After cooling to desired temperature in flowing air, the samples were exposed to reactant mixture (5000 ppm CO in air) at a constant temperature. After holding this temperature for 30 min, it was stepwise increased to the next designed temperature. The FTIR spectra were recorded every 20 °C (from 20 to 160 °C) after 30 min of steady state reaction.

Results and discussion

CO oxidation activity over TiO_2 supported catalysts

Fig. 1 shows the CO oxidation activities over a series of TiO_2 supported catalysts prepared by photodeposition and the activity order is observed as Co/TiO_2 > Cu/TiO_2 > Mn/TiO_2 > Ni/TiO_2 > V/TiO_2 > Cr/TiO_2 > Fe/TiO_2 (all catalysts activated at 400 °C). Co/TiO_2 exhibits the best activity and 100% CO conversion could be obtained at temperatures below 15 °C. However, the activity drops gradually with reaction time, indicating the quick deactivation of Co/TiO_2 catalyst (not shown here). For Cu/TiO_2, a 50% CO conversion is obtained at 50 °C and a 100% CO conversion is obtained at 95 °C. The activity of Cu/TiO_2 is remarkable high when compared to other Cu catalysts under similar reaction conditions.[15–19] Mn/TiO_2 and Ni/TiO_2 catalysts also exhibit high activity and overall CO oxidation could be obtained at below 200 °C. To our knowledge, Ni and Mn are not popular active components during the past researches on CO oxidation and it is the first time to report highly active Mn/TiO_2 and Ni/TiO_2 catalysts. From Fig. 1, it is seen that quite good CO oxidation activities can be achieved on some

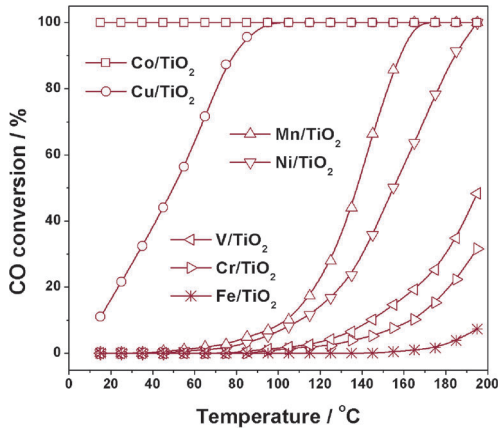

Fig. 1 Catalytic activities for CO oxidation on TiO_2 supported catalysts prepared by photo-deposition. Reaction conditions: 0.2 g catalyst, 5000 ppm CO, air balance, GHSV = 24 000 h^{-1}.

TiO_2 supported catalysts prepared by photodeposition. The great success of these catalysts may be ascribed to the advanced preparation method and the proper activation process. Since Cu/TiO_2 appears to be very promising catalyst for CO oxidation, a detailed study on Cu/TiO_2 will be presented in the following sections.

CO oxidation activity over different Cu/TiO_2 catalysts

Fig. 2 presents the CO oxidation activity of Cu/TiO_2 activated at 200, 400 and 600 °C, respectively. It is seen that the activation temperature shows significant effect on CO oxidation over Cu/TiO_2 prepared by photodeposition and by wet impregnation. For Cu/TiO_2 prepared by photodeposition, the samples activated at 600 °C and 400 °C show almost identical activity and they both show much higher activity than that activated at 200 °C. While for Cu/TiO_2 prepared by wet impregnation, the sample activated at 400 °C shows the highest activity, followed by the sample activated at 200 °C and the lowest activity is observed on the sample activated at 600 °C.

The effects of activation temperature on CO oxidation over Cu/TiO_2 catalysts can be ascribed to the change in the states of

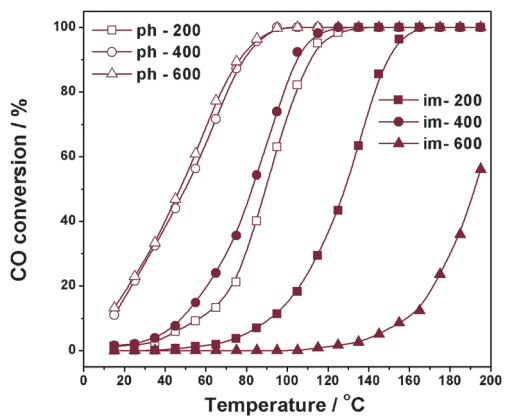

Fig. 2 Catalytic activities for CO oxidation on Cu/TiO_2 prepared by photodeposition or impregnation, and activated at different temperatures. Reaction conditions: 0.2 g catalyst, 5000 ppm CO, air balance, GHSV = 24 000 h^{-1}.

active copper species during activation process, similar to those reported for cobalt-based catalysts.[22,23] From Fig. 2, it is also seen that Cu/TiO_2 catalyst prepared by photodeposition exhibits much better CO oxidation activity than that prepared by wet impregnation activated at the same temperature. The good activity and stability of Cu/TiO_2 prepared by photodeposition demonstrates its great potential for future application.

Effect of reaction conditions on CO oxidation over Cu/TiO_2

The effects of GHSV and initial CO concentration on CO oxidation activity over Cu/TiO_2 prepared by photo-deposition are shown in Fig. 3. The CO conversion drops gradually with increasing GHSV from 12 000 h^{-1} to 48 000 h^{-1}. Nevertheless, an overall CO oxidation to CO_2 is obtained at below 150 °C even at the highest GHSV of 48 000 h^{-1}. Under fixed GHSV of 24 000 h^{-1}, a slight decrease in CO conversion is observed on Cu/TiO_2 catalyst with initial CO concentration increasing from 1000 ppm to 5000 ppm, and a more serious decrease in CO conversion is observed with CO concentration further increasing to 10 000 ppm.

Kinetic for CO oxidation over Cu/TiO_2

The Arrhenius plots of CO oxidation on different Cu/TiO_2 catalysts are shown in Fig. 4. The apparent activation energy for CO oxidation on Cu/TiO_2 prepared by photodeposition is

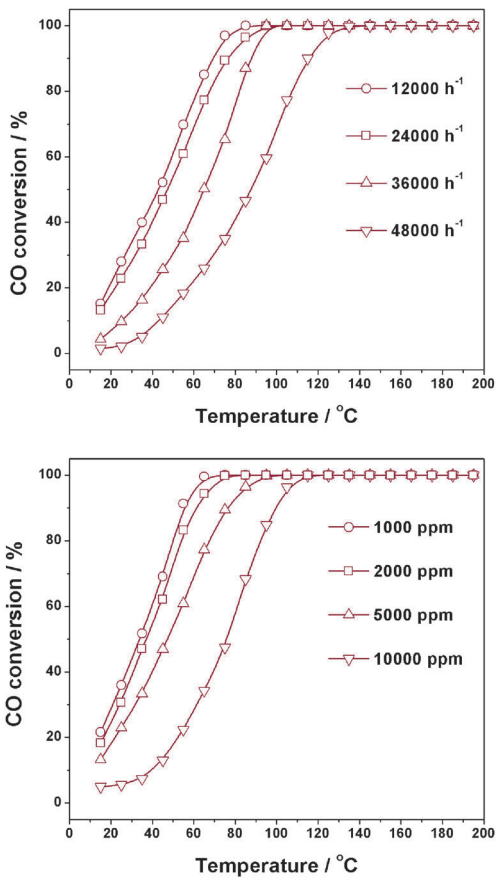

Fig. 3 Effects of GHSV and initial CO concentration on CO oxidation activity over Cu/TiO_2 catalyst.

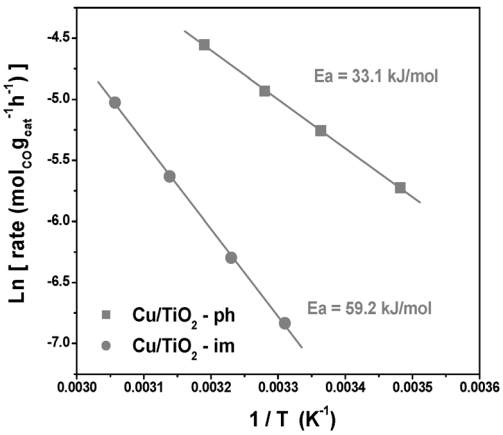

Fig. 4 Arrhenius plot of CO oxidation on Cu/TiO_2 catalysts activated at 400 °C for 1 h.

as low as 35.5 kJ mol^{-1}, while the apparent activation energy on Cu/TiO_2 prepared by wet impregnation is 59.2 kJ mol^{-1}. Notablely, the pre-exponential A on Cu/TiO_2-ph (7.64×10^3 s^{-1}) is much lower than that on Cu/TiO_2-im (1.87×10^7 s^{-1}), indicating the effective active sites on Cu/TiO_2-ph are much less than that on Cu/TiO_2-im. The CO oxidation reaction rate on Cu/TiO_2 is governed by apparent activation energy. The formation of different copper species on TiO_2 support is proposed to be responsible for the kinetics difference of Cu/TiO_2 prepared by different methods.

Characterization of Cu/TiO_2 catalysts

The XRD patterns of different Cu/TiO_2 samples are shown in Fig. 5. Typical diffraction peaks of TiO_2 support corresponding to anatase (JCPDS 21-1272) and rutile (JCPDS 21-1276) phase are observed in all Cu/TiO_2 samples. Besides, diffraction peaks at 13.1° and 33.6° corresponding to $Cu(OH)_2$ (JCPDS 42-0746) can be found in as-prepared Cu/TiO_2-im. Through activation at 400 °C, the $Cu(OH)_2$ transforms to CuO (JCPDS 41-0254), as illustrated by the diffraction peak at 35.5°. Based on the above observation, it is deduced that copper species adsorb on TiO_2 support in the form of $Cu(OH)_2$ during wet impregnation and then transform to CuO during activation process. For Cu/TiO_2 by photo-deposition, diffraction peaks at 43.2° and 50.3° corresponding to metallic Cu (JCPDF 04-0836), are observed in the as-prepared sample. Through activation, the intensities of diffraction peaks corresponding to metallic Cu decrease, while no new diffraction peaks appear. It is easily seen that some of metallic Cu has transformed to other copper species, probably Cu_2O and/or CuO, during activation. However, the main diffraction peak of Cu_2O (JCPDF 65-3288), *e.g.* the peak at 36.2°, cannot be distinguished due to overlapped by the diffraction peaks of TiO_2 support.

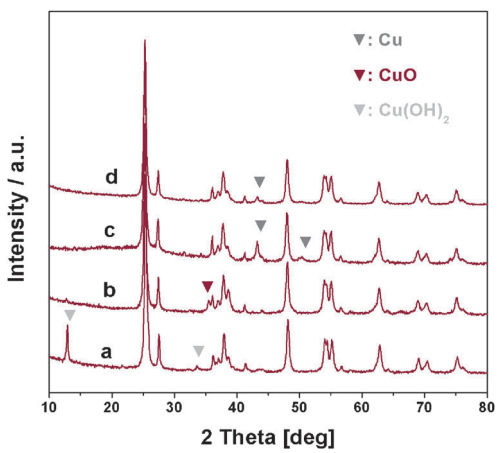

Fig. 5 XRD patterns of different Cu/TiO_2 samples. (a) as-prepared Cu/TiO_2-im, (b) Cu/TiO_2-im activated at 400 °C for 1 h, (c) as-prepared Cu/TiO_2-ph and (d) Cu/TiO_2-ph activated at 400 °C for 1 h.

The TEM images of Cu/TiO_2 prepared by wet impregnation and by photo-deposition are shown in Fig. 6. It is seen that similar spherical clusters with diameters of 3–6 nm are observed to disperse on the TiO_2 support. So, the cluster size, distribution and morphology of copper species should not be the key factors controlling the catalytic activity.

Fig. 7 shows the X-ray photoelectron and Auger electronic spectra of Cu/TiO_2 prepared by wet impregnation and photo-deposition. For Cu/TiO_2-ph, the binding energy of 932.5 and 952.3 eV is observed in Cu 2p region, associated with the Cu^0 and/or Cu^I_2O.[24] Meanwhile, the kinetic energy of 913 eV associated with Cu^I_2O and/or $Cu^{II}O$,[25] together with kinetic energy of 914.5 eV associated with Cu^0, is observed. Based on the results from both X-ray photoelectron and Auger electronic spectra, the Cu species in Cu/TiO_2-ph should exist in the form of Cu^I_2O and Cu^0. For Cu/TiO_2-im, the binding energy of 932.5, 934.4, 952.3 and 954.0 eV is observed in the Cu 2p region. The binding energy of 934.4 and 954.0 eV is associated with $Cu^{II}O$, while binding energy of 932.5 eV and 952.3 eV is associated with the Cu^0 and/or Cu^I_2O. The absence of kinetic energy of 914.5 eV in Auger electronic spectra excludes the existence of Cu^0, so the Cu species in Cu/TiO_2-im should exist in the form of Cu^I_2O and $Cu^{II}O$. Based on the areas of deconvoluted Cu 2p3/2 XPS peak, *ca.* 60% of copper species are in the form of Cu^I_2O and *ca.* 40% copper species are in the form of $Cu^{II}O$.

The different Cu species on TiO_2 are further investigated by means of temperature-programmed reduction and the H_2-TPR profiles of Cu/TiO_2 are shown in Fig. 8. Since the TiO_2 support is almost irreducible at below 400 °C, the reduction peaks in this temperature range correspond to the reduction of different types of copper oxides. For Cu/TiO_2-ph,

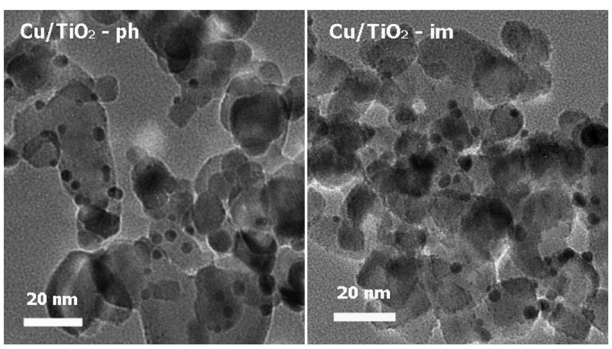

Fig. 6 TEM images of Cu/TiO_2 prepared by different methods and activated at 400 °C for 1 h.

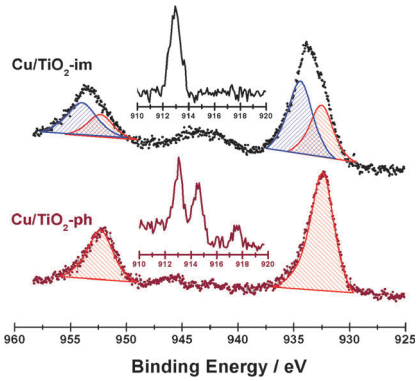

Fig. 7 X-Ray photoelectron and Auger electronic spectra (inset) of Cu/TiO_2 prepared by different methods and activated at 400 °C for 1 h.

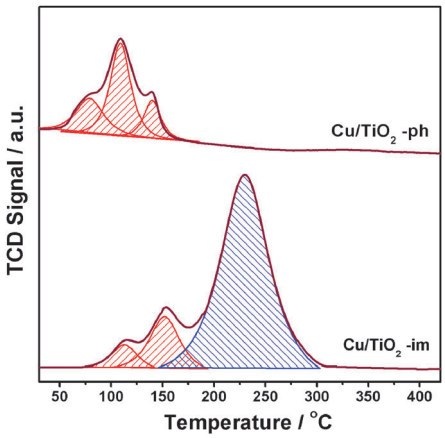

Fig. 8 H_2-TPR profiles of Cu/TiO_2 prepared by different methods and activated at 400 °C for 1 h.

three reduction peaks centered at 80, 110 and 140 °C can be observed, corresponding to the reduction of various Cu_2O on TiO_2.[16] While for Cu/TiO_2-im two peaks at 110 and 150 °C corresponding to the reduction of Cu_2O are observed. Besides, a reduction peak at centered at 240 °C is observed and assigned to the reduction of crystalline CuO.[18] For a quantitative analysis, the H_2 consumption of each reduction peak and corresponding quantity of copper oxides are carefully calculated. For Cu/TiO_2-im, Cu(I) is 395.8 μmol g^{-1} and Cu(II) is 741.5 μmol g^{-1}, as displayed in Table 1. Based on the total copper loading of 1126.5 μmol g^{-1}, we determine that copper species exist in the form of oxides, 35% Cu_2O and 65% CuO. It should be mentioned that a slightly higher proportion of Cu_2O is obtained from XPS analysis (40%) than that from TPR analysis (35%). As is known, XPS is surface analysis technique with detection depth of several nanometres, while TPR is bulk analysis technique. The different quantitative results from XPS and TPR analysis therefore indicate the slight enrichment of Cu_2O species in Cu/TiO_2-im, which is formed during activation process. While for Cu/TiO_2-ph, part of copper exists in the form of Cu(I) (733.8 μmol g^{-1}, *ca.* 65%) and the rest of copper (*ca.* 35%) should exist in the form of Cu^0.

Transformation of copper species on TiO_2

Based on above characterization results, the transformation of copper species in Cu/TiO_2 prepared by different methods is proposed. For Cu/TiO_2-im, copper species adsorb on the surface of TiO_2 support in the form of $Cu(OH)_2$ after wet impregnation. During activation at 400 °C, the decomposition of $Cu(OH)_2$ to CuO takes places and some of CuO species are reduced to Cu_2O species due to the existence of CO in the reactant gas mixture. As a result, Cu_2O–CuO/TiO_2 is the final product we obtained after activation. While for the preparation of Cu/TiO_2 by photodeposition, a much more complicated process is involved as follows:

$$Cu^{2+}{}_{aq} \rightarrow Cu^{2+}{}_{ads}$$

$$TiO_2 + h\nu \rightarrow TiO_2 + e^- + p^+$$

$$Cu^{2+}{}_{ads} + 2\,e^- \rightarrow Cu^0{}_{ads}$$

$$mCu^0{}_{ads} \rightarrow Cu_m$$

First, the copper cations in aqueous solution adsorb on the surface of TiO_2. Under the ultraviolet irradiation ($h\nu \geq E_g$ = 3.02 eV), electron-hole pairs are also created on the surface of TiO_2. The adsorbed copper cations are subsequently reduced to copper atoms by the photo-induced electrons ($E^0_{Cu2+/Cu}$ = −1.25 eV) and then agglomerate to form copper nano-clusters on TiO_2. During activation, parts of metallic Cu species are oxidized to Cu_2O (*ca.* 35%) in oxidizing conditions, while the rests are preserved in the metallic form. On the whole, Cu–Cu_2O/TiO_2 is obtained as the final product after activation.

CO adsorption on Cu/TiO_2 at room temperature

Fig. 9 presents the time-resolved FTIR spectra of CO adsorption on Cu/TiO_2 at room temperature. In the normal carbonyls region, a strong band at 2105 cm^{-1} and a weak band at 2060 cm^{-1} are observed on Cu/TiO_2 prepared by impregnation, which significantly increase in intensity with adsorption time. The band at 2105 cm^{-1} is attributed to the mono-carbonyl group on Cu^+ while that at 2060 cm^{-1} is attributed to mono-carbonyl on metallic Cu.[26–28] Besides,

Table 1 H_2 consumption during TPR of Cu/TiO_2 catalysts

	Reduction peaks									
Catalyst	*T*/°C	H_2/μmol g^{-1}	*T*/°C	H_2/μmol g^{-1}	*T*/°C	H_2/μmol g^{-1}	Cu(I)/μmol g^{-1}	Cu(II)/μmol g^{-1}	Sum[a]/μmol g^{-1}	Cu^{0b}/μmol g^{-1}
Cu/TiO_2-ph	80	105.5	110	183.9	140	77.5	733.8	—	1101.5	367.7
Cu/TiO_2-im	110	69.6	150	128.3	240	741.5	395.8	741.5	1126.5	—

[a] Analyzed by ICP. [b] Cu^0 = Sum–Cu(I)–Cu(II).

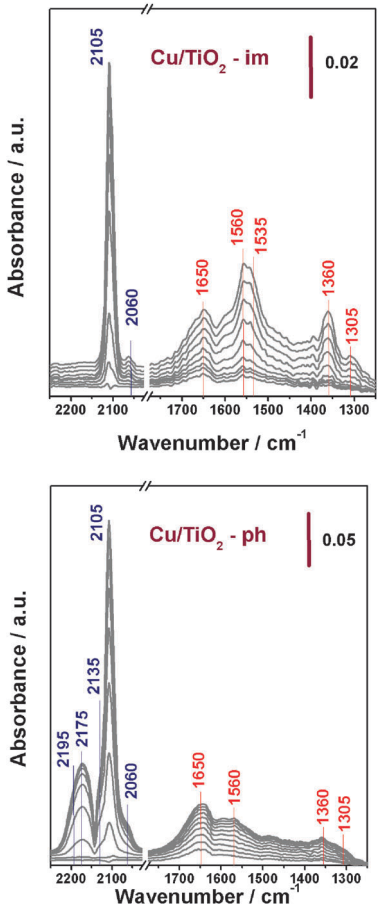

Fig. 9 Time-resolved FTIR spectra of CO adsorption on Cu/TiO_2 prepared by different methods at room temperature.

some other bands at 1650, 1560, 1535, 1360 and 1305 cm^{-1} are observed and their intensities also increase with the adsorption time. These bands are attributed to the products of reactive CO adsorption, *e.g.* carbonates, bicarbonates, carboxylates or formates.[29,30] The FTIR spectra of CO adsorption on Cu/TiO_2-im indicate that CO predominantly adsorbs on Cu^{2+} cationic center, accompanied by the reduction of Cu^{2+} to Cu^+ and Cu^0 ($E^0_{Cu2+/Cu+}$ = 0.153 eV; $E^0_{Cu2+/Cu}$ = −1.25 eV). Since carbonyls of Cu^{2+} are not detectable at room temperature, the IR bands we observed are carbonyls of Cu^+ and Cu^0 together with products of reactive CO adsorption.

In the case of Cu/TiO_2-ph, CO adsorption proceeds in some other way. As seen in Fig. 9, a strong band at 2105 cm^{-1} corresponding to Cu^+–CO and a weak band 2060 cm^{-1} corresponding to Cu^0–CO are observed, similar to the results on Cu/TiO_2-im. Besides, bands at 2135, 2175 and 2195 cm^{-1} corresponding to polycarbonyls of Cu^+, *e.g.* $Cu^+(CO)_2$ and $Cu^+(CO)_3$,[30] can be clearly observed in the carbonyls region. Because Cu^+ cannot be reduced to Cu^0 at room temperature with high $E^0_{Cu+/Cu}$ of −2.53 eV, the Cu^0–CO should be originated from CO adsorption on already-existed Cu^0 on TiO_2. In contrast, the band corresponding to Cu^0–CO observed on Cu/TiO_2-im is originated from CO adsorption on newly-formed Cu^0 reduced from Cu^{2+}. The Cu^+–CO observed on Cu/TiO_2-ph is originated from CO adsorption on already-existed Cu^+ and hence polycarbonyls of Cu^+ are observed on Cu/TiO_2-ph. Based on the above observations, it is indicated that both Cu^+ and Cu^0 in Cu/TiO_2 prepared by photo-deposition are accessible and CO molecular adsorb as carbonyls on both Cu^+ and Cu^0, followed by the oxidation of carbonyls.

In situ FTIR spectra of CO oxidation on $Cu–Cu_2O/TiO_2$

The results of IR bands observed on Cu/TiO_2 prepared by photo-deposition, *i.e.* $Cu–Cu_2O/TiO_2$, under steady-state $CO–O_2$ reaction conditions are shown in Fig. 10. At 20 °C, a strong band at 2105 cm^{-1} corresponding to Cu^+–CO and a weak band 2060 cm^{-1} corresponding to Cu^0–CO together with broad bands centered at 2170 cm^{-1} corresponding to $Cu^+–(CO)_x$ are observed in the carbonyls region. Meanwhile, a series of bands in the region of below 1700 cm^{-1} are observed. Briefly, band at 1650 cm^{-1} is assigned to bidentate carbonates,[31] while the bands at 1495 and 1305 cm^{-1} are assigned to monodentate carbonates.[29] The bands at 1560 and 1350 cm^{-1} are assigned to formates,[32] formed through the interaction between CO and surface hydroxyls. The bands at 1535 and 1390 cm^{-1} is assigned to carboxylates,[29] while the band at 1605 cm^{-1} is assigned to bi-carbonates.[33] It is seen that CO predominantly adsorbs on the Cu^+ site in $Cu–Cu_2O/TiO_2$ and the formed carbonyls can be oxidized even at room temperature. With increasing temperature from 20 °C to 120 °C, the intensity of IR bands associated with carbonyls decreases gradually. Considering that the carbonyls on Cu^+ are quite stable at below 200 °C,[30] the decrease in the intensity of IR bands is mainly attributed to the consumption of carbonyls. Meanwhile, the intensity of IR band corresponding to bidentate carbonates also decreases with increasing temperatures. However, in contrast, the intensity of IR bands associated with formates and carboxylates increases gradually, indicating the accumulation of these species. Based on the above observations, we propose that the carbonyls on Cu^+ are initially oxidized to bidentate carbonates, which finally transform to CO_2.

CO oxidation mechanism on $Cu–Cu_2O/TiO_2$

By means of a series of different characterization techniques, the exact composition of Cu/TiO_2 prepared by photo-deposition is well defined as $Cu–Cu_2O/TiO_2$. In the early work

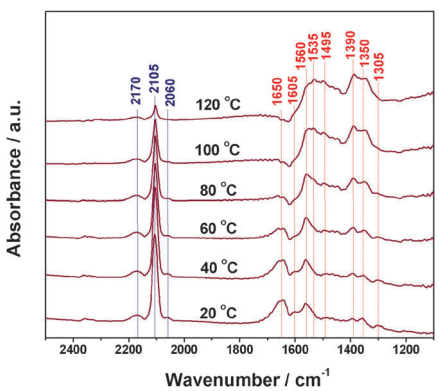

Fig. 10 *In situ* FTIR spectra of CO oxidation on Cu/TiO_2 catalyst prepared by photodeposition.

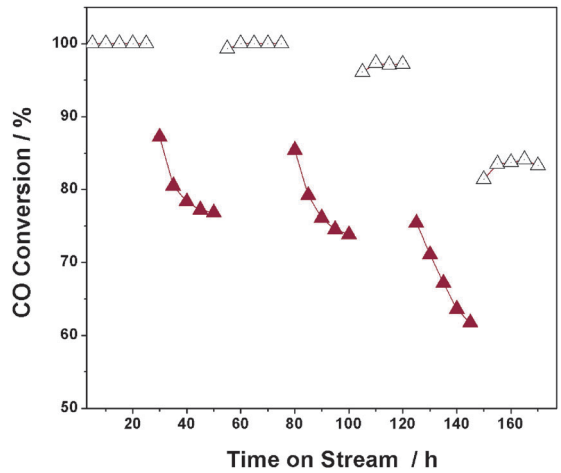

Fig. 11 Time-on-stream behaviour of Cu–Cu_2O/TiO_2 catalyst for CO oxidation at 100 °C. Reaction conditions: 0.2 g catalyst, 5000 ppm CO, 0 (hollow symbol) or 2% (filled symbol) H_2O, balance air, GHSV = 24 000 h^{-1}.

of Jernigan and Somorjai,[12] quite different activation energy for CO oxidation was observed over copper catalysts with different oxidation states (Cu: 37.1 kJ mol^{-1}; Cu_2O: 58.8 kJ mol^{-1}; CuO: 71.4 kJ mol^{-1}). In this work, the apparent activation energy for CO oxidation on Cu–Cu_2O/TiO_2 is determined to be 33.1 kJ mol^{-1} and therefore, Cu_2O should not be the actual active sites for reaction. For more precise information, the detailed CO oxidation pathway is described as follows.

First, the CO–O_2 reaction over copper catalyst is of Langmuir-Hinshelwood type where adsorbed CO reacts with adsorbed oxygen and the following elementary reactions are considered:

$$CO + * \rightarrow CO*$$

$$O_2 + * \rightarrow O_2*$$

$$O_2* + * \rightarrow 2O*$$

$$CO* + O* \rightarrow CO_2 + 2*$$

The adsorption of CO and O_2 are fast reaction in equilibrium and the adsorption entropies are dependent on the type of adsorption sites. For CO, the adsorption entropy is much greater on Cu_2O than that on metallic copper [34] and as a consequence CO prefers to adsorb on the Cu^+ cation site with σ bonding and π back-bonding synergistic effect. This is also proved by the FTIR results (Fig. 10) where Cu^+–CO is observed as key reaction intermediate. However, the kinetic results indicate that Cu_2O should not be the active sites for CO oxidation. Since both metallic Cu and Cu_2O are accessible in Cu–Cu_2O/TiO_2, we propose that CO oxidation proceeds through the cooperation of Cu_2O and Cu. The apparent activation energy E_{App} for CO oxidation can be obtained as $E_{App} = E_{LH} + E_{dis} + E_{diff} - E_{CO} - E_{O2}$. Herein, E_{LH} is the barrier for Langmuir-Hinshelwood reaction and E_{dis} is the barrier for oxygen dissociation. E_{CO} and E_{O2} are the adsorption energy of CO and O_2, respectively. E_{diff} is the energy barrier for adsorbed CO diffusing from Cu_2O to Cu or adsorbed O diffusing from Cu to CuO_2. It should be mentioned that E_{diff} might be varied in a large range, determined by the diffusion pathway and surface coverage. If the Langmuir–Hinshelwood reaction occurs at the borders between Cu_2O and metallic copper, the E_{diff} may be very small, or even can be neglected. Thus, the formula is approximately simplified as $E_{App} = E_{LH} + E_{dis} - E_{CO} - E_{O2}$. The cooperation between Cu_2O and metallic Cu contributes to the low apparent activation energy of 33.1 kJ mol^{-1} for CO oxidation. Meanwhile, since very limited borders between Cu_2O and Cu is available in Cu–Cu_2O/TiO_2, very low pre-exponential A of 7.64×10^3 s^{-1} is obtained on Cu–Cu_2O/TiO_2.

Durability of Cu–Cu_2O/TiO_2 for CO oxidation

The durability of Cu–Cu_2O/TiO_2 catalyst under different reaction conditions is further studied. No deactivation can be observed on Cu–Cu_2O/TiO_2 after 200 h reaction at 100 °C in the absence of H_2O (not shown in the figure), suggesting the good stability of catalyst under dry conditions. However in contrast, the presence of 2% H_2O in the reaction stream results in an obvious decrease in the CO conversion from 100% to 76%, as seen in Fig. 11. After turning off the H_2O supply, the CO conversion on Cu–Cu_2O/TiO_2 gradually recovers to 100%. Turning on the H_2O supply again results in more serious deactivation of catalyst and the CO conversion cannot recover to the initial level (100%) after turning off the H_2O supply. Based on these observations, two types of catalyst deactivation by H_2O are proposed. One type of deactivation is due to the competitive adsorption of H_2O on the active sites, which inhibits the adsorption of CO and O_2. Generally, this type of deactivation is impermanent and easily recovered. The other type of deactivation is caused by the H_2O-promoted oxidation of Cu or Cu_2O. Obviously, this type of deactivation is permanent and irreversible.

Conclusions

The catalytic oxidation of CO over a series of Me/TiO_2 catalysts (Me : TiO_2 = 1 : 10) prepared by photodeposition was investigated. Cu/TiO_2 exhibited remarkably high activity with low apparent activation energy of 33.1 kJ mol^{-1} and a detailed study was carried out on Cu/TiO_2 catalyst. The exact composition of Cu/TiO_2 prepared by photo-deposition was determined to be Cu–Cu_2O/TiO_2, based on the characterization results from XRD, XPS-AES, H_2-TPR and FTIR of CO adsorption. The CO oxidation over Cu–Cu_2O/TiO_2 was investigated by *in situ* FTIR spectra and carbonyls on Cu^+ were observed as key intermediates. The mechanism for CO oxidation over Cu–Cu_2O/TiO_2 was further discussed and the step of Langmuir-Hinshelwood reaction ($CO* + O* \rightarrow CO_2 + 2*$) was proposed to occur through the cooperation between Cu_2O and metallic copper. Time-on-stream behaviour of Cu–Cu_2O/TiO_2 for CO oxidation indicated no deactivation at 100 °C for over 200 h in the absence of H_2O. While in the presence of 2% H_2O, two types of deactivation was observed, which was then attributed to the competitive adsorption of H_2O on the active sites and H_2O-promoted oxidation of Cu or Cu_2O.

Acknowledgements

This work is financially supported by the National Basic Research Program of China (2009CB623502) and MOE (IRT0927). L. L. thanks the support from the State Key Laboratory of Catalytic Materials and Reaction Engineering (RIPP, SINOPEC).

References

1 M. Haruta, S. Tsubota, T. Kobayashi, H. Kageyama, M. J. Genet and B. Delmon, *J. Catal*., 1993, **144**, 175.
2 G. C. Bond and D. T. Thompson, *Gold Bullet*., 2000, **33**, 41.
3 M. Comotti, W. C. Li, B. Spliethoff and F. Schüth, *J. Am. Chem. Soc*., 2006, **128**, 917.
4 T. Schalow, B. Brandt, M. Laurin, S. Schauermann, J. Libuda and H. J. Freund, *J. Catal*., 2006, **242**, 58.
5 B. T. Qiao, L. Q. Liu, J. Zhang and Y. Q. Deng, *J. Catal*., 2009, **261**, 241.
6 J. Jansson, M. Skoglundh, E. Fridell and P. Thormählen, *Top. Catal*., 2001, **16/17**, 385.
7 J. Jansson, A. E. C. Palmqvist, E. Fridell, M. Skoglundh, L. Osterlund, P. Thormählen and V. Langer, *J. Catal*., 2002, **211**, 387.
8 F. Grillo, M. M. Natile and A. Glisenti, *Appl. Catal., B*, 2004, **48**, 267.
9 M. M. Yung, E. M. Holmgreen and U. S. Ozkan, *Catal. Lett*., 2007, **118**, 180–186.
10 M. J. Pollard, B. A. Weinstock, T. E. Bitterwolf, P. R. Griffiths, A. P. Newbery and J. B. Paine III, *J. Catal*., 2008, **254**, 218.
11 K. I. Choi and M. A. Vannice, *J. Catal*., 1991, **131**, 22.
12 G. G. Jernigan and G. A. Somorjai, *J. Catal*., 1994, **147**, 567.
13 F. H. M. Dekker, M. C. Dekker, A. Bliek, F. Kapteijn and J. A. Moulijn, *Catal. Today*, 1994, **20**, 409.
14 B. White, M. Yin, A. Hall, D. Le, S. Stolbov, T. Rahman, N. Turro and S. O'Brien, *Nano Lett*., 2006, **6**, 2095.
15 C. S. Chen, J. H. You, J. H Lin and Y. Y. Chen, *Catal. Commun*., 2008, **9**, 2381.
16 H. Q. Wan, Z. Wang, J. Zhu, X. W. Li, B. Liu, F. Gao, L. Dong and Y. Chen, *Appl. Catal., B*, 2008, **79**, 254.
17 J. L. Cao, Y. Wang, X. L. Yu, S. R. Wang, S. H. Wu and Z. Y. Yuan, *Appl. Catal., B*, 2008, **79**, 26.
18 J. L. Cao, Y. Wang, T. Y. Zhang, S. H. Wu and Z. Y. Yuan, *Appl. Catal., B*, 2008, **78**, 120.
19 V. A. Sadykov, S. F. Tikhov, N. N. Bulgakov and A. P. Gerasev, *Catal. Today*, 2009, **144**, 324.
20 J. M. Herrmann, J. Disdier and P. Pichat, *J. Phys. Chem*., 1986, **90**, 6028.
21 L. D. Li, Q. Shen, J. Cheng and Z. P. Hao, *Appl. Catal., B*, 2010, **93**, 259.
22 W. H. Yang, M. H. Kim and S. W. Ham, *Catal. Today*, 2007, **123**, 94.
23 C. W. Tang, C. C. Kuo, M. C. Kuo, C. B. Wang and S. H. Chien, *Appl. Catal., A*, 2006, **309**, 37.
24 H. J. Choi and M. Kang, *Int. J. Hydrogen Energy*, 2007, **32**, 3841.
25 S. Y. Lee, N. Mettlach, N. Nguyen, Y. M. Sun and J. M. White, *Appl. Surf. Sci*., 2003, **206**, 102.
26 K. Hadjiivanov and H. Knozinger, *Phys. Chem. Chem. Phys*., 2001, **3**, 1132.
27 D. Scarano, S. Bordiga, C. Lamberti, G. Spoto, G. Ricchiardi, A. Zecchina and C. O. Areán, *Surf. Sci*., 1998, **411**, 272.
28 F. Boccuzzi, A. Chiorino, G. Martra, M. Gargano, N. Ravasio and B. Carrozzini, *J. Catal*., 1997, **165**, 129.
29 A. Davydov, *IR Spectroscopy Applied to Surface Chemistry of Oxides*, Nauka, Novosibirsk, 1984.
30 K. I. Hadjiivanov and G. N. Vayssilov, *Adv. Catal*., **47**, 307.
31 A. Dandekar and M. A. Vannice, *J. Catal*., 1998, **178**, 621.
32 M. Kantcheva, M. U. Kucukkal and S. Suzer, *J. Catal*., 2000, **190**, 144.
33 K. I. Hadjiivanov and G. Busca, *Langmuir*, 1994, **10**, 4534.
34 D. F. Cox and K. H. Schulz, *Surf. Sci*., 1991, **249**, 138.

